

Insights into the synergy of zero-valent iron and copper oxide in persulfate oxidation of Orange G solutions

Chenxi Wang^{1,2} · Jinqun Wan^{1,2,3} ·
Yongwen Ma^{1,2,3} · Yan Wang^{1,2}

Received: 6 October 2014 / Accepted: 25 March 2015 / Published online: 17 April 2015
© Springer Science+Business Media Dordrecht 2015

Abstract The degradation of Orange G (OG) by persulfate (PS, $S_2O_8^{2-}$) activated with dual catalysts that combined zero-valent iron (ZVI) and copper oxide (CuO) was investigated through batch experiments. Effects of pH, initial OG concentration, persulfate dosages, and dosages of dual catalysts on OG degradation were also examined. Higher persulfate concentration and catalysts dosages resulted in higher OG degrading rates. The OG degradation was higher under acidic conditions (pH 3.0 and 5.0) when compared to alkaline conditions. The constituents and the morphology of the catalysts coating before and after reaction were also investigated with X-ray diffraction and scanning electron microscopy. Radical mechanism was studied and three radical scavengers [methanol (MA), tert-butanol (TBA), phenol] were used to determine the type of major active species taking part in the degradation of OG. It was assumed that the SO_4^- or $HO\cdot$ played a major role in the OG degradation. In conclusion, the ZVI/CuO/PS system is a good candidate for use in detoxifying water contaminants.

Keywords Persulfate · Zero valent iron (ZVI) · CuO · Dual catalysts · Orange G

✉ Jinqun Wan
ppjqwan@scut.edu.cn

¹ School of Environment and Energy, South China University of Technology, Guangzhou 510006, People's Republic of China

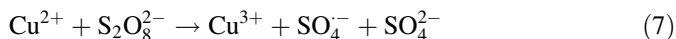
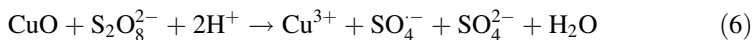
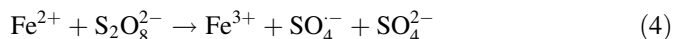
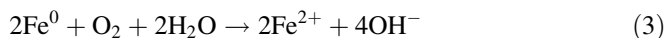
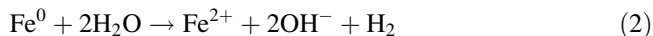
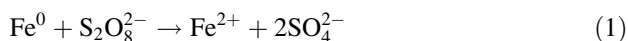
² The Key Lab of Pollution Control and Ecosystem Restoration in Industry Clusters, Ministry of Education, Guangzhou 510006, People's Republic of China

³ State Key Lab Pulp and Paper Engineering, South China University of Technology, Guangzhou 510640, People's Republic of China

Introduction

Dying industries produce a large amount of wastewater that contains oxidized recalcitrant, toxic, and non-biodegradable compounds [1, 2]. Azo dyes represent 50 % of all commercial dyes due to their chemical stability and simple synthesis process [3]. Azo dyes characterized by the presence of nitrogen-to-nitrogen double bonds ($-\text{N}=\text{N}-$) have received increasing attention not only because of their color, but also on account of their potentially carcinogenic intermediates [4]. They are abated by some wastewater treatment technologies such as adsorption, biological processes, and membrane filtration, in which dyes cannot be completely mineralized [5–7].

In recent years, advanced oxidation processes (AOPs) have been proven effective to treat biorefractory and toxic organics [8–10]. Currently, as an active species with a redox potential ($E_0 = 2.5 - 3.1$ vs. NHE) [11], sulfate radicals ($\text{SO}_4^{\cdot-}$) can destroy most of the organics in water [12]. In the presence of PS, $\text{SO}_4^{\cdot-}$ can be generated under activation conditions of UV, heat, high pH, activated carbon, phenols, and transition metal ions [13–19]. Recently, some researches used Orange G (OG), Reactive Orange 122 (RO122), and methylene blue as target compound to investigate the degradation ability in the system activated persulfate by Fe(II), Fe(III), UV, and heat [20–22]. Since PS activation by UV and heat takes much energy, using transition metal ions to activate persulfate has been widely developed as an efficient and promising method to treat organic compounds [23]. Many transition metals such as Fe(II) and Cu(II) can efficiently activate persulfate to produce sulfate radicals as follows (Eqs. 1–7) [24, 25].



Because the homogeneous catalysis (Fe^{2+}/PS , Cu^{2+}/PS) has a high amount of dissolved iron, which may cause an excess dosage of catalysts, zero valent iron (ZVI)- and copper oxidate-activated persulfate to produce sulfate radicals is a promising alternative. The use of solid catalysts such as ZVI and copper oxidate not only overcome the waste of catalyst, but also avoid the disadvantage of bringing in other ions by metal salts.

However, few studies have investigated the degradation of organics by persulfate activation with mixed catalysts [26]. Also, information of degradation of dye wastewater using activated persulfate activated with dual solid catalysts is lacking.

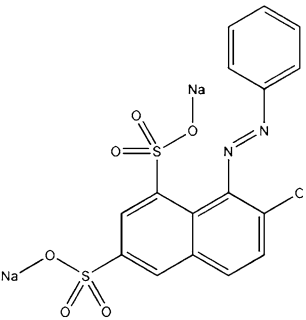
To improve the understanding of interaction between two kinds of catalysts. Orange G is a typical azo dye in textile wastewater and has commonly been used as a model compound for the degradation of dyes [27–29]. The degradation of the model organic compound OG in aqueous solution by CuO and ZVI catalyzed PS oxidation is studied in this paper. The research objective is to gain insight into the following questions. (1) Does there exist a synergistic effect between CuO and ZVI? How do the operational conditions (PS concentration, dual catalysts dosage, initial pH and temperature) affect the OG degradation? (2) What change of catalyst will be before and after reaction? (3) Which kind of active species play a part in the degradation process? Can the active species mineralize the organic contaminant?

Materials and methods

Materials

Unless otherwise indicated, all chemicals used in this study were reagent grade. Ultrapure water was produced using a Millipore Milli-Q system. The ZVI (purity > 99 %, approx. 150 μm) was obtained from Aladdin Chemistry Co., Ltd (Shanghai, China). As determined by N_2 isothermal adsorption (the BET surface area), the total surface of these ZVI were 0.389 m^2/g . The nano-CuO (purity > 99 %, approx. 50 nm) was obtained from Aladdin Chemistry Co., Ltd (Shanghai, China). Orange G (purity > 99 %, the characteristics of OG is shown in Table 1) was purchased from Aladdin Chemistry Co., Ltd (Shanghai, China). Sodium persulfate ($\text{Na}_2\text{S}_2\text{O}_8$, 98 %) was obtained from Fuchen Chemical Co., Ltd.

Table 1 Characteristics of OG

Dye	Structure	Molecular formula	MW (g mol^{-1})	λ_{max}
Orange G		$\text{C}_{16}\text{H}_{10}\text{N}_2\text{Na}_2\text{O}_7\text{S}_2$	452	478

The phenol (C_6H_5OH , 99 %), methanol (CH_3OH , 98 %), and tert-Butanol ($C_4H_{10}O$, 98 %) were purchased from Kermel Chemical Reagent Co., Ltd. Potassium iodide (KI, 99 %) was obtained from Tianda Chemical Reagent Co., Ltd. Sodium bicarbonate ($NaHCO_3$, 99.5 %) was purchased from Kermel Chemical Reagent Co., Ltd. Sodium hydroxide (NaOH, 96 %) and sulfuric acid (H_2SO_4 , 98 %) were purchased from the Second Guangzhou Chemical Reagent Factory.

In this study, the concentration of OG solution was 0.2 mM and the concentration of persulfate was 2 mM. The pH condition of the system ranged from 3 to 11. The pH was controlled by adjusting the solution by adding 0.1 M sulfuric acid (H_2SO_4) and sodium hydroxide (NaOH) every 10 min (pH degree change was less than 0.2).

Experimental procedure

Stock solution of OG (0.2 mM) and persulfate (2 mM) was prepared by adding a required amount of pure OG and persulfate sodium. Batch experiments were conducted in a 250 mL serum bottles opened to the atmosphere and shaken at 150 rpm in a rotary shaker (ZHWHY-20102C, Shanghai, China) at 25 ± 0.2 °C. For determining the effect of the dosages of the catalyst on the degradation of OG, 0.01, 0.05, 0.1, 0.2 g/L ZVI and nano-CuO were studied, respectively. All samples were withdrawn in the predetermined time intervals by ethanol, an agent well-known for quenching sulfate radicals [23], and the residual catalysts were separated by centrifugation for 5 min at 10,000 rpm in 2 mL polypropylene microcentrifuge tubes, then the supernatant was filtered through a 0.45- μ m membrane filter and analyzed for OG, dissolved Fe^{2+} , dissolved Cu^{2+} and persulfate. The initial pH values of all solutions were adjusted with 1 M sodium hydroxide (NaOH) or sulfuric acid (H_2SO_4). The ZVI surface composition was studied by scanning electron microscopy (SEM).

Analytical methods

Analysis of degradation of OG

The UV–Vis absorbance of the samples was analyzed with a UV2301 II spectrophotometer (Shanghai, China). The degradation of OG was determined by measuring the maximum absorbance at 478 nm. The mineralization of OG solution was determined by total organic carbon (TOC) content and analyzed by using a TOC analyzer (Shimadzu) after the sample was quenched by 2 M sodium thiosulfate pentahydrate.

Measurements of persulfate and metal ion

The concentration of persulfate anion was determined by spectrophotometric determination with potassium iodide [30]; total iron and ferrous iron were measured with 1,10-phenanthroline at a wavelength of 510 nm by using a UV–Vis spectrophotometer (UV2301II, Shanghai, China) [31]. The copper ion was quantified using a Shimadzu AA-6300C Atomic Absorption Spectrophotometer.

The pH was monitored by pH meter (Shanghai LeiCi PHS-25) equipped with a pH electrode. The ORP was monitored by pH meter (Shanghai LeiCi PHS-25) equipped with an oxidation electrode potential electrode(ORP).

SEM

The morphology of ZVI and nano-CuO was observed by the thermal field emission scanning electron microscope (FESEM, Quanta 200, Netherlands) manufactured by Oxford Instruments Ltd. The specimens were coated with an electrically conductive surface layer of Au.

XRD

In order to analyze the surface of ZVI and nano-CuO before and after reaction, ZVI and nano-CuO particles were rinsed with N_2 -sparged acetone and ultrapure water several times and then dried at 60 °C inside a vacuum drying oven. The crystallographic structures of the oxides were determined by an X-ray diffractometer D8 Advance X-ray Diffraction system and Bruker AXS with a copper target tube radiation (Cu K α 1) producing X-rays at a wavelength of 0.15418 nm. Samples were put on a quartz plate

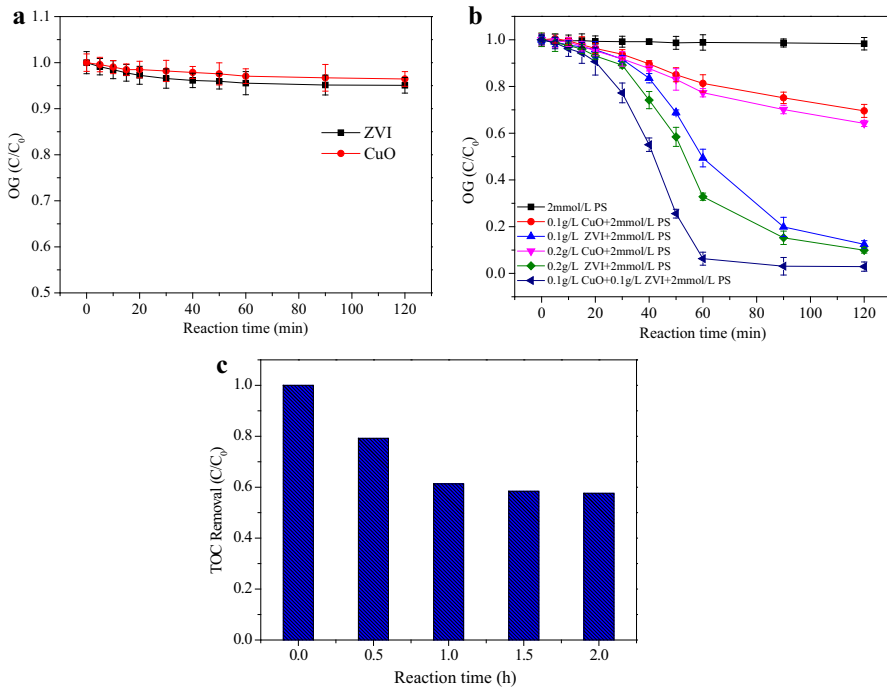


Fig. 1 **a** Adsorption of OG on ZVI and CuO, **b** degradation of OG in different systems, **c** TOC removal of OG in ZVI/CuO/PS system. Experimental condition: $[OG]_0 = 0.2$ mM; $[PS]_0 = 2$ mM; ZVI = 0.1 g/L; CuO = 0.1 g/L; $T = 25$ °C; $pH = 5.0 \pm 0.2$

and were scanned from 15 to 80 (2θ) at scan speed of $1.2^\circ \text{ min}^{-1}$, a scan step of 0.02° , 1.0DS-SS slits, a 8.0-mm RS slit for monochromator.

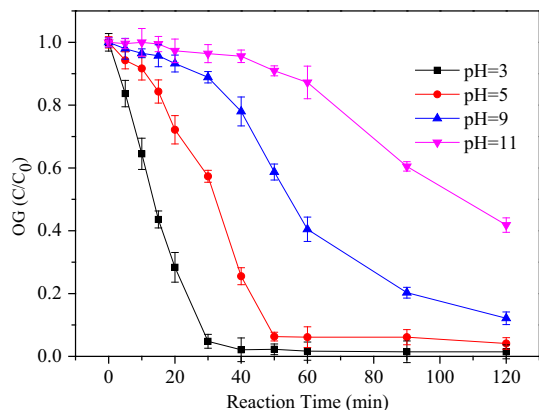
Results and discussion

Degradation of OG in different systems

The adsorption of OG on ZVI and CuO is shown in Fig. 1a; the results revealed ZVI and CuO had only a few OG adsorption ($<5\%$). To investigate the decolorization effect of the ZVI/CuO/PS system, all of the decolorization processes of OG in different systems are compared in Fig. 1b. The results showed that no decolorization was observed in the mere presence of persulfate. In addition, activation of PS by ZVI or CuO were also investigated, and the results showed that approximately 18% of the OG was removed over 60 min in CuO/PS system, and about 50% of the OG was eliminated from solution over 1 h in ZVI/PS system. When the concentration of CuO and ZVI increased to 0.2 g/L, the decolorization of OG improved to 22.7 and 67.2% in CuO/PS and ZVI/PS systems, respectively. Furthermore, more than 90% of the OG was removed with ZVI/CuO activated persulfate, reflecting that dual catalysts made a difference for decolorization of OG. However, due to several intermediate products of OG coupled with toxicity and potential carcinogenicity, the TOC removal of OG (Fig. 1c) was an important indicator of the degradation of OG.

As presented in Fig. 1c, although the OG degradation was almost more than 95% in the ZVI/CuO/PS system within 1 h, the reduction of TOC was only 38.7%. The removal of OG and TOC kept rising during 1 h reaction time and level off afterwards. The reason should be that intermediate compounds which were difficult to mineralize were produced continually during the reaction time. It was clearly shown that the ZVI- and CuO-activated persulfate, on the one hand, removed the color of OG completely, on the other hand, mineralized the intermediate products of OG. Fe^{2+} and Cu^{2+} were the main species that can activate persulfate to produce

Fig. 2 Effect of initial pH in the degradation of OG.
Experimental condition:
[OG] $_0$ = 0.2 mM;
[PS] $_0$ = 2 mM; ZVI = 0.1 g/L;
CuO = 0.1 g/L; T = 25 °C



sulfate radicals [23]. ZVI and CuO played the role of source for Fe^{2+} and Cu^{2+} . Additionally, the redox reaction between Fe^{3+} , Fe^0 and Cu^{2+} also enhanced the activation of persulfate.

Degradation of OG under different initial pH

The OG degradation with an initial concentration (C_0) of 0.2 mM under the different initial pH is shown in Fig. 2. As pH value plays a prominent role in the degradation of organics, the reaction was carried out at initial pH 3.0, 5.0, 9.0, 11.0, respectively. At different initial pH, the order in the degradation of OG in the ZVI/CuO/PS system was studied: (initial pH 3) > (initial pH 5) > (initial pH 7) > (initial pH 11). As shown in Fig. 2, the fastest removal rate of OG in the ZVI/CuO/PS combined system appeared at initial pH 3.0. With the increase of pH, the efficiency of degradation of OG declined, indicating that the OG degradation preferred acidic pH to neutral and alkaline condition. This result agreed with Xu et al. [32], who suggested that the precipitation of Fe^{3+} ions occurred when $\text{pH} > 4.0$. Also, the strong hydrolysis of Cu^{2+} in neutral or alkaline condition may inhibit persulfate activation [26]. The formation of Fe^{2+} complexes could impede the further catalytic reaction between Fe^{2+} and persulfate. The reaction can be described by Eq. (8) [33].

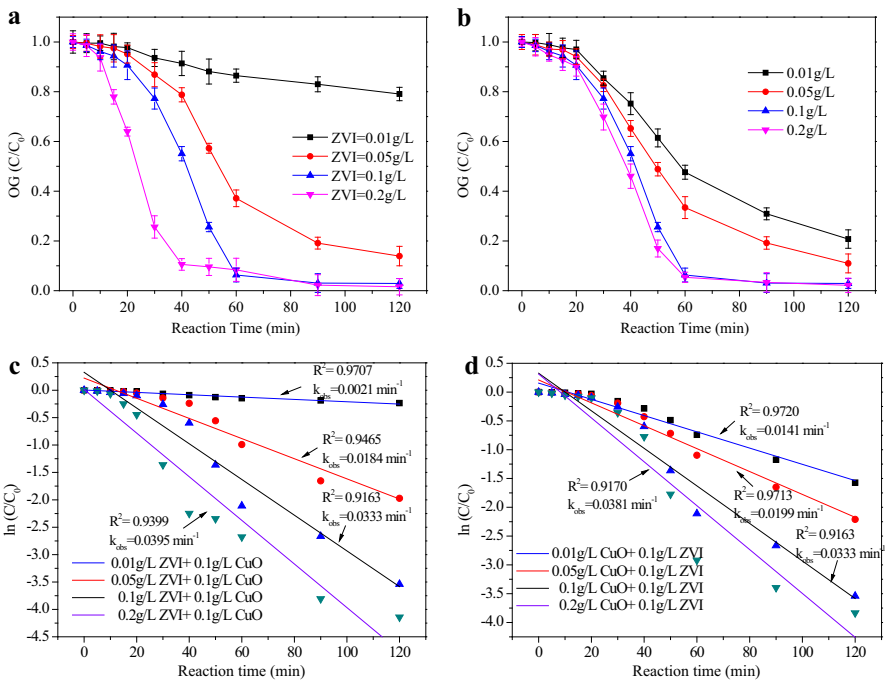
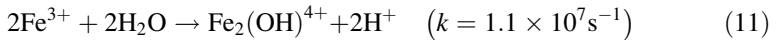
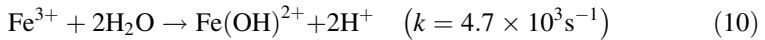
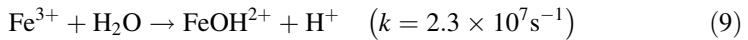
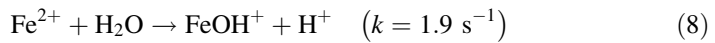
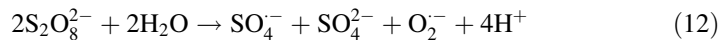


Fig. 3 Effect of catalyst dosage in the degradation of OG. **a** ZVI, $[\text{CuO}] = 0.1 \text{ g/L}$, **b** CuO, $[\text{ZVI}] = 0.1 \text{ g/L}$, **c** reaction kinetic plots for the degradation of OG versus time with different dosages of ZVI, **d** reaction kinetic plots for the degradation of OG versus time with different dosages of CuO. Experimental condition: $[\text{OG}]_0 = 0.2 \text{ mM}$; $[\text{PS}]_0 = 2 \text{ mM}$; $T = 25 \text{ }^\circ\text{C}$; $\text{pH} = 5.0 \pm 0.2$

Also, the hydrolysis products of Fe^{3+} (FeOH^{2+} , $\text{Fe}_2(\text{OH})^{4+}$, and $\text{Fe}(\text{OH})_3$) accumulated near the surface of ZVI blocked the heterogeneous catalytic reaction. The formation of hydrolysis products are shown in the following Eqs. (9)–(11).



Moreover, persulfate activation mechanisms may be different in different pH conditions. While the metal ion activation can be the dominant mechanism under acidic conditions, the base-activated persulfate may be the primary mechanism at high pH values. The base activation mechanism has been affirmed as follows in Eq. (12) [34].



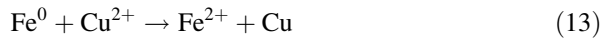
Effect of ZVI and CuO dosage

Figure 3 shows the effect of catalyst dosage on the OG degradation by ZVI and CuO catalyzed PS oxidation. With the increase of ZVI and CuO dosage, the removal ratio improved. concentrations of ZVI and CuO 0.01, 0.05, 0.1, 0.2 g/L were added respectively. Figure 3a shows that the degradation efficiency of OG was 20.92, 87.1, 97.1, 98.41 % with ZVI dosages of 0.01, 0.05, 0.1, 0.2 g/L, respectively, after a 2-h reaction. Figure 3b shows the degradation order of OG in the ZVI/CuO/PS system at different concentrations of CuO: (CuO 0.2 g/L) > (CuO 0.1 g/L) > (CuO 0.05 g/L) > (CuO 0.01 g/L). After 1 h, the degradation rate of OG tends to be similar to the dosage of CuO between 0.1 and 0.2 g/L.

Table 2 Rate constants of ZVI and CuO activated persulfate oxidation of OG under various dosages of catalysts

Conditions	k_{obs} (min^{-1} or mg/L^{-1})	R^2	Reaction order
ZVI, 0.01 g/L CuO, 0.1 g/L	0.0021	0.9707	Pseudo first-order
ZVI, 0.05 g/L CuO, 0.1 g/L	0.0184	0.9465	Pseudo first-order
ZVI, 0.1 g/L CuO, 0.1 g/L	0.0333	0.9163	Pseudo first-order
ZVI, 0.2 g/L CuO, 0.1 g/L	0.0395	0.9399	Pseudo first-order
ZVI, 0.1 g/L CuO, 0.01 g/L	0.0141	0.9720	Pseudo first-order
ZVI, 0.1 g/L CuO, 0.05 g/L	0.0199	0.9713	Pseudo first-order
ZVI, 0.1 g/L CuO, 0.1 g/L	0.0333	0.9163	Pseudo first-order
ZVI, 0.1 g/L CuO, 0.2 g/L	0.0381	0.9170	Pseudo first-order

The activation of persulfate by dual catalysts was due to the release of Fe^{2+} and Cu^{2+} in the ZVI/CuO/PS system. During the reaction, Fe^{2+} was continuously supplied to the activation of persulfate, at the same time, a substitution reaction occurred between Fe^0 and Cu^{2+} which also provided Fe^{2+} as shown in the following Eq. (13). From the perspective of complete mineralization of pollutants, the sustained activity of ZVI and Cu^{2+} to activate persulfate may also have better control of the reaction process. To achieve the highest degradation efficiencies of OG, the dosage of ZVI 0.1 and CuO 0.1 g/L was chosen as the optimum condition.

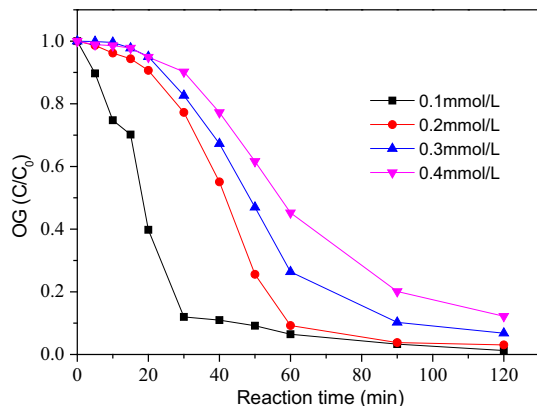


The observed rate constants (k_{obs}) of the degradation of OG in contact with dosages of ZVI and CuO were investigated (Fig. 3c, d). As indicated in Table 2, the pseudo first-order degradation kinetics applied well to all experiments in the ZVI/CuO/PS system. It was evident from the values of k_{obs} (Table 2) that the rate constants increased by increasing the dosages of ZVI from 0.0021 to 0.0395 mg/L $^{-1}$ min $^{-1}$. Similar results were obtained by increasing the dosage of CuO from 0.01 to 0.2 g/L, and as a consequence, the rate constant elevated from 0.0141 to 0.0381 mg/L $^{-1}$ min $^{-1}$. When the amount of catalyst was doubled to 0.2 g/L, the increase in of the OG degradation rate was not notable (the kinetic constant increase from 0.0333 to 0.0395). Allowing for the effective utilization rate of catalysts and eco-friendly, the optimum concentration of ZVI and CuO in this study were chosen as 0.1 g/L, respectively.

Effect of OG initial concentration

The effect of OG initial concentration on the degradation of OG in the dual catalysts system with the presence of persulfate is shown in Fig. 4. It can be seen that with the OG initial concentration increase from 0.1 to 0.4 mmol/L, the degradation rate declined. At the condition of confined amount of persulfate, effective sulfate radicals were limited and organic compounds competed for free sulfate radicals.

Fig. 4 Effect of OG initial concentration in the degradation of OG. Experimental condition: $[\text{PS}]_0 = 2 \text{ mM}$; $[\text{ZVI}]_0 = 0.1 \text{ g/L}$; $[\text{CuO}] = 0.1 \text{ g/L}$; $T = 25 \text{ }^\circ\text{C}$; $\text{pH} = 5.0 \pm 0.2$



Under the same oxidation system conditions, such as amount of catalysts, pH value, PS concentration, the number of reactive radical species generated by the process was assumed constant [35]. Thus, at high OG concentration, the similar amounts of oxidant used in the ZVI/CuO/PS system constituted a limiting factor in the consumption of active species, and its efficiency would be reduced at higher OG concentration.

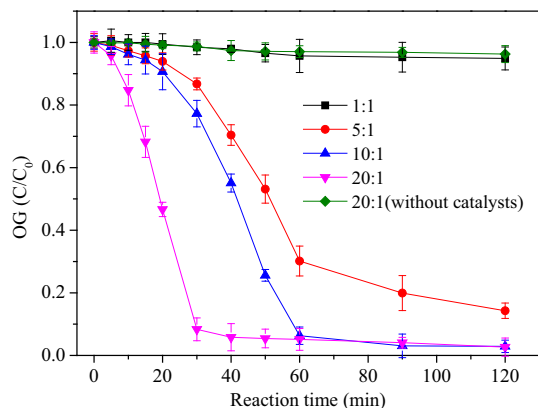
Effect of PS initial concentration

As a source of active species, persulfate is an important factor in the ZVI/CuO/PS system. The effect of persulfate concentration on OG degradation was investigated by changing the ratios (PS:OG) from 1:1 to 20:1. The result showed that degradation of OG reached a few degrees only in the system that has PS with high concentrations ($[PS]_0: [OG]_0 = 20:1$, without catalysts). As shown in Fig. 5, when the dosage of persulfate increased from 1:1 to 10:1 (PS:OG), the degradation of OG increased from 4.4 to 93.7 % within a 60 min reaction. However, in comparison with OG degradation when the PS:OG molar ratio increased to 20:1, there was an obvious accelerating effect in the ZVI/CuO/PS system during 60 min, but resulted in only a slight increase in the OG removal after 1 h. This phenomenon suggested that there was too much excess persulfate to produce sulfate free radicals when the persulfate concentration increased beyond a numeric value, which was similar to the results of Hori et al. and Chu et al. [36, 37]. Also, it was reported that sulfate radicals ($SO_4^{\cdot-}$), produced in the activation of PS, reacted with excessive PS to form SO_4^{2-} described in Eq. (14) [38]. Under an optimum condition ($[PS]_0 = 2$ mM, $[ZVI] = 0.1$ g/L, $[CuO] = 0.1$ g/L and pH 3), the OG ($[OG]_0 = 0.2$ mM), degradation in the ZVI/CuO/PS system was achieved by 95 % in 60 min.



The results from Figs. 4 and 5 strongly suggested that the degradation of OG proceeded more quickly with increasing PS/OG molar ratio, and OG oxidation was

Fig. 5 Effect of PS dosage in the degradation of OG.
Experimental condition:
 $[OG]_0 = 0.2$ mM;
 $[ZVI]_0 = 0.1$ g/L;
 $[CuO] = 0.1$ g/L; $T = 25$ °C;
pH = 5.0 ± 0.2



more susceptible to the influence of this factor than the initial OG concentration. These conclusions were also demonstrated in previous studies by other researchers at various PS and pollutant initial concentrations [39].

Iron and copper leaching and persulfate decomposition

The oxidation reduction potential electrode (ORP) played an important role in the decomposition of organic compounds [40]. As shown in Fig. 6a, in the ZVI/CuO and CuO/PS systems, the ORP values were essentially flat; the same phenomenon appeared in the aqueous solution that only had persulfate. But in the ZVI/PS and ZVI/CuO/PS systems, the ORP values changed drastically, due to the consumption of persulfate. The increased ORP values in the ZVI/PS and ZVI/CuO/PS systems indicated a highly oxidative condition which is because of more production of sulfate radicals [41, 42].

Ferrous (Fe^{2+}), ferric ions and copper ions are deemed to be important reagents in the homogeneous persulfate oxidation system. To elucidate the effect of dual catalysts in the ZVI/CuO/PS system, the variation of Fe^{2+} , dissolved iron and copper ions concentration during the reaction time were investigated. Figure 6c showed that the concentration of Fe^{2+} and dissolved iron went up from 0 to 24 mg/L

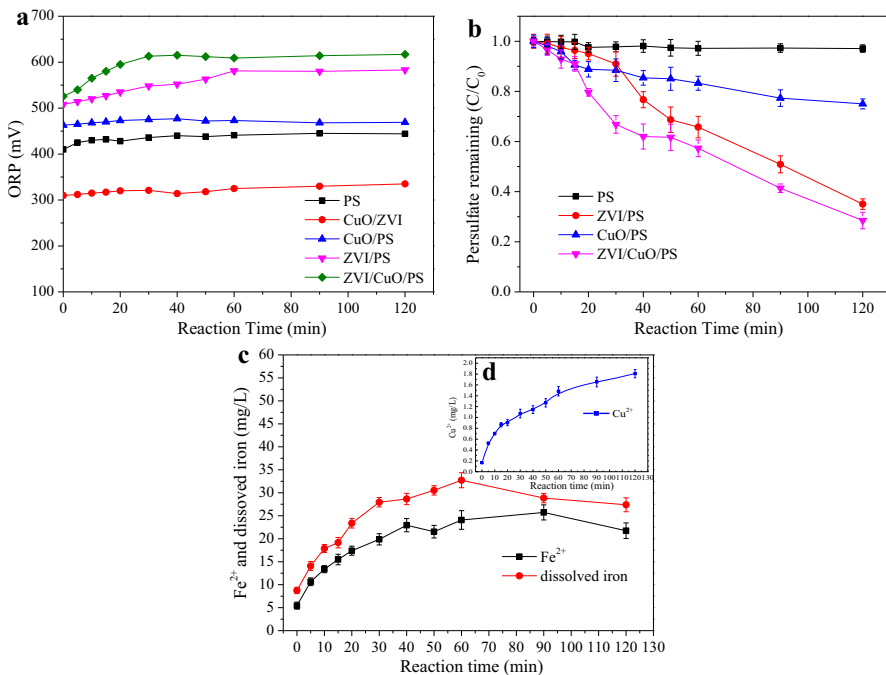


Fig. 6 a The ORP versus time, b the persulfate decomposition during reaction time, c iron leaching during reaction time, d inset graph is the copper ion leaching during reaction time. Experimental condition: $[\text{OG}]_0 = 0.2 \text{ mM}$; $[\text{ZVI}]_0 = 0.1 \text{ g/L}$; $[\text{CuO}] = 0.1 \text{ g/L}$; $T = 25 \text{ }^\circ\text{C}$; $[\text{PS}]_0 = 2 \text{ mM}$; $\text{pH} = 5.0 \pm 0.2$

and 32 mg/L during 1 h reaction time, respectively. However, the enhancement of Fe^{2+} would increase the reaction rate. After 1 h, both concentrations of Fe^{2+} and dissolved iron began to maintain a stable value while it was not obvious on the degradation of OG. That may be on account of the disadvantageous reaction between SO_4^- and excess Fe^{2+} as shown in Eq. (15), leading to a lower removal of the organic contaminants. In aqueous solution, the copper ion also increased from 0 mg/L to 1.808 mg/L during the reaction time, which had a comparable catalytic ability to Fe^{2+} . Moreover, copper ions activating persulfate had a stable and continuous degradation effect in aqueous solution [26]. The addition of CuO plays an important role that not only was a source of Cu^{2+} , but also produced

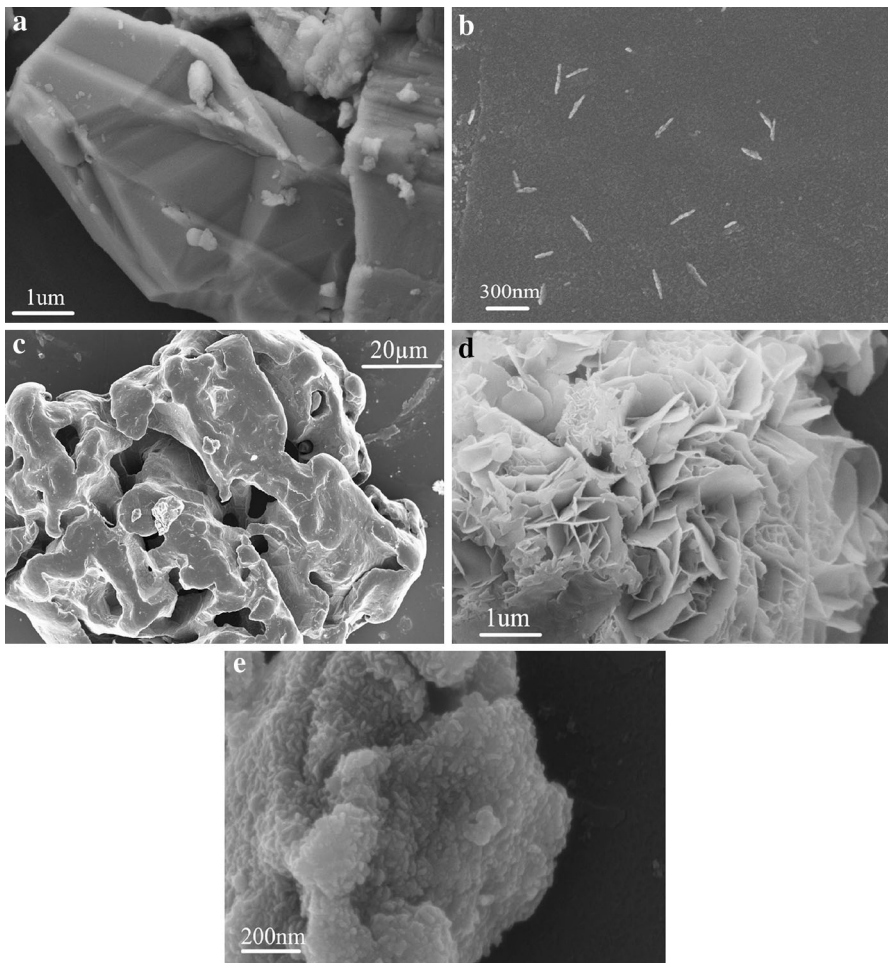
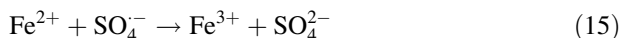


Fig. 7 FE-SEM images of **a** original ZVI, **b** original CuO, **c** ZVI after 30 min reaction at pH 5.0, **d** ZVI and CuO 60 min reaction at pH 5.0, **e** ZVI and CuO 90 min reaction at pH 5.0

heterogeneous catalysis. Both Fe^{2+} and Cu^{2+} promoted the decomposition of persulfate and generated free sulfate radicals.



As shown in Fig. 6, the concentration of Fe^{2+} and Cu^{2+} were reached to 27.4 and 1.8 mg/L, respectively. However, Chinese national effluent discharge standard had no clear discharge limit on iron, but the copper discharge standard in wastewater is 2.0 mg/L. Thus, the discharge of metal concentration could meet the standard.

Characterization of catalyst surface

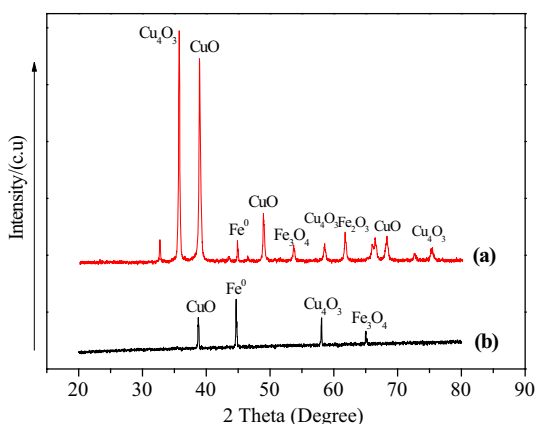
SEM

In order to investigate the morphology and structure of the ZVI and CuO products before and after oxidation in the aqueous solution, the morphology of the ZVI and CuO obtained before and after oxidation was clearly visible from the SEM images shown in Fig. 7a–e. The original ZVI showed large particles with sizes at around tens of microns with relatively smooth surface. As shown in Fig. 7b, generally, the image of CuO before reaction displayed some rod-like, acicular substances. Compared with the original ZVI, the surface of the ZVI appeared some pores (Fig. 7c). After a 60 min reaction with persulfate and OG, the SEM image of ZVI and CuO presented a big aggregation composed of a sheet substance (Fig. 7d). However, it can be seen that the iron and copper corrosion products were mixed corrosion products ranging from needle-like or flake-like crystals to amorphous masses (Fig. 7e).

X-ray powder diffraction

The XRD patterns of catalysts containing ZVI and CuO obtained before and after oxidation reaction are presented in Fig. 8. The diffraction peaks of these catalysts

Fig. 8 XRD patterns of catalysts obtained before and after reaction. (a) catalysts before reaction; (b) catalysts after reaction. Experimental condition: $[\text{OG}]_0 = 0.2 \text{ mM}$; $[\text{ZVI}]_0 = 0.1 \text{ g/L}$; $[\text{CuO}] = 0.1 \text{ g/L}$; $T = 25 \text{ }^\circ\text{C}$; $[\text{PS}]_0 = 2 \text{ mM}$; $\text{pH} = 5.0 \pm 0.2$

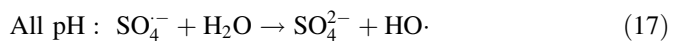


match well with the characteristic signals of Fe_2O_3 crystals 64.0° , Fe_3O_4 crystals 65.0° and Fe^0 crystals 44.7° , thus indicating the formation of Fe_2O_3 , Fe_3O_4 , and Fe^0 . Also, Fig. 8 shows that the peaks at $2\theta = 35.5^\circ, 38.7^\circ, 48.7^\circ, 61.5^\circ, 66.2^\circ$, and 68° may be corresponding to CuO (PCPDF File no. 80-1917) and the other peaks at $2\theta = 35.6^\circ, 58^\circ$, and 75° may be corresponding to Cu_4O_3 (PCPDF File no. 83-1665). We found that the catalysts before oxidation reaction were Fe^0 , CuO , Cu_3O_4 , Fe_2O_3 , and Fe_3O_4 . After catalytic reaction with persulfate, the key component of catalysts was Fe^0 , CuO , Cu_3O_4 , and Fe_3O_4 .

Radical mechanism

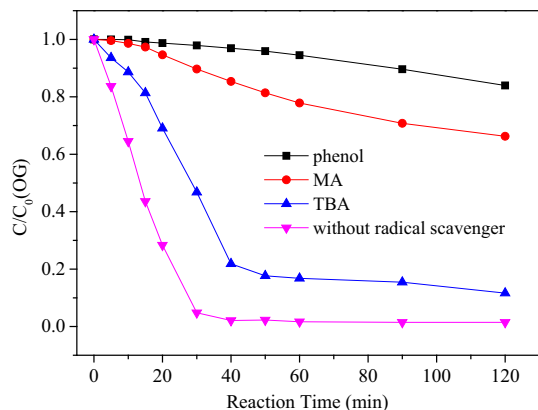
From the above, persulfate was primarily activated by ZVI and CuO and produced sulfate free radicals ($\text{SO}_4^{\cdot-}$). Under the acid condition, especially at pH 3, the sulfate free radical ($\text{SO}_4^{\cdot-}$) was mainly formed by reaction between Fe^{2+} , Cu^{2+} , and persulfate (Eqs. 4, 7). When the pH increased to 5, the concentration of Fe^{2+} and Cu^{2+} decreased due to the reduction of H^+ . On the other hand, persulfate reacted directly with ZVI and CuO to produce activated species (Eqs. 1, 6). In previous studies, it was reported that sulfate free radical ($\text{SO}_4^{\cdot-}$) was the primary active species at acidic conditions; nevertheless, hydroxyl radical ($\text{HO}\cdot$) was the main radical at alkaline conditions [43].

In addition, the sulfate free radical ($\text{SO}_4^{\cdot-}$) may convert to the hydroxyl radical ($\text{HO}\cdot$), a mechanism that can be confirmed to be as follows (Eqs. 16, 17) [44]:



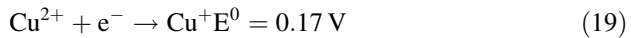
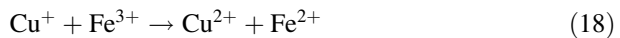
To investigate which kind of radical species mainly play a part in the dual catalysis reaction, the radical mechanism was studied in this part using chemical probe. In the previous studies, phenol, methanol (MA), and tert-Butanol (TBA) were used as the chemical probe of $\text{HO}\cdot$ and $\text{SO}_4^{\cdot-}$ in the advanced oxidation systems [17]. Figure 9 shows the effect of different radical scavengers (phenol, methanol, and,

Fig. 9 Effect of different radical scavengers on the degradation of OG.
Experimental condition:
[OG]₀ = 0.2 mM;
[PS]₀ = 2 mM; [radical scavenger] = 200 mM;
[ZVI]₀ = 0.1 g/L; [CuO] = 0.1 g/L; T = 25 °C;
pH = 5.0 ± 0.2



tert-Butanol) on the degradation of OG. It is thoroughly proved that all three (phenol, MA, and TBA) are effective quenching agents for HO· ($k_{\text{phenol}/\text{HO}\cdot} = 6.6 \times 10^9 \text{ M}^{-1}\text{S}^{-1}$, $k_{\text{MA}/\text{HO}\cdot} = 1.2 \times 10^9 - 2.8 \times 10^9 \text{ M}^{-1}\text{S}^{-1}$, $k_{\text{TBA}/\text{HO}\cdot} = 3.8 \times 10^8 - 7.6 \times 10^8 \text{ M}^{-1}\text{S}^{-1}$) and $\text{SO}_4^{\cdot-}$ ($k_{\text{phenol}/\text{SO}_4^{\cdot-}} = 8.8 \times 10^9 \text{ M}^{-1}\text{S}^{-1}$, $k_{\text{MA}/\text{SO}_4^{\cdot-}} = 1.6 \times 10^7 - 7.7 \times 10^7 \text{ M}^{-1}\text{S}^{-1}$, $k_{\text{TBA}/\text{SO}_4^{\cdot-}} = 4 \times 10^5 - 9.1 \times 10^5 \text{ M}^{-1}\text{S}^{-1}$) [12, 17, 45]. However, the inhibiting effects of OG degradation were not obvious when TBA was added into the ZVI/CuO/PS system, whereas MA has a more inhibiting effect than TBA. When phenol was added into the ZVI/CuO/PS system, the degradation of OG was almost stopped. The main active species that plays an important role in the ZVI/CuO/PS combined system was the sulfate free radical ($\text{SO}_4^{\cdot-}$) or hydroxyl radical ($\text{HO}\cdot$).

The proposed activation of PS by ZVI and CuO included both homogeneous and heterogeneous activation. Ji et al. [46] reported phenol degradation by using CuO to activate peroxymonosulfate in aqueous solution and assumed that the activation of peroxymonosulfate was triggered by the redox pair of Cu(II)/Cu(I). Therefore, we speculate that the highly catalytic activity of dual catalysts involved the activation of PS mediated by both redox pairs of Cu(II)/Cu(I) and Fe(III)/Fe(II) species in a dual catalysts system. According to the conclusion of Nie et al., the reduction of Fe^{3+} by Cu^+ is thermodynamically favorable as shown in the following equations [47]:



As mentioned above, persulfate may be primarily activated by ZVI, involving the formation of Fe^{2+} , especially at low pH values (both on the surface of ZVI and in the solution), and sulfate free radicals ($\text{SO}_4^{\cdot-}$). During the reaction, copper oxidate also played an important role in activation of persulfate, resulting in the generation of Cu^{3+} , Cu^{2+} , and activate species. In addition, Fe^{2+} and Cu^{2+} were high-

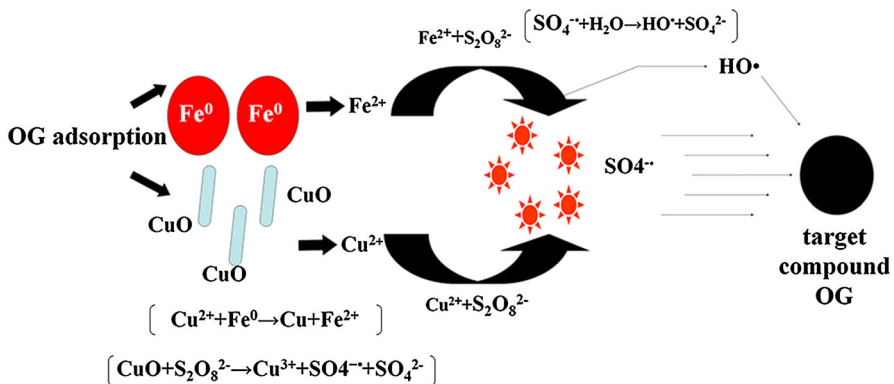


Fig. 10 Mechanism of the activation of persulfate in the ZVI/CuO/PS combined system

efficiency catalysts in accelerating persulfate to generate sulfate radicals. However, in the ZVI/CuO/PS system, four mechanisms led to thorough degradation and substantial mineralization of OG: (1) the adsorption of OG on catalysts (only a few), (2) the activation of PS by ZVI and CuO to generate SO_4^- , (3) the activation of Fe^{2+} and Cu^{2+} to produce SO_4^- , (4) SO_4^- transformed to $\text{HO}\cdot$, and both attacked the target compound (Fig. 10).

Conclusion

The study investigated the applicability of dual catalysts combined ZVI- and nano-CuO-activated persulfate oxidation for degradation of OG. This advanced oxidation process has been demonstrated to be highly effective in producing sulfate free radicals for the treatment of OG. Not only was the ZVI/CuO/PS combined system effective in OG degradation, but it also had good mineralization. The effects of the initial pH, catalyst dosage, oxidant dosage, and initial compound concentration have been evaluated. The optimum ZVI dosage was 0.1 and 0.1 g/L for CuO. The dual catalysts system has advantages compared with the system which only has one catalyst. These results were caused by features of Fe^{2+} and Cu^{2+} and the synergistic effect between ZVI and CuO.

This study also has important implications for the interaction between ZVI and CuO in the dual catalysts system. The results obtained from the characterization methods of SEM and XRD revealed that the redox reaction and replacement reaction between ZVI and CuO can affect the decomposition of persulfate, which as a result could influence the degradation of OG. However, further studies will be performed to the mechanism of this interaction. The results of these investigations provide important insights into the development of advanced oxidation process for treatment of textile dyes. The excessive intake of copper by human may lead to headaches, increased heart rate, and hair loss [48]. In order to promote the process for application, toxicity tests are needed. For the purpose of balancing pros and cons, the accurate dosing of catalysts and oxidants is crucial.

Acknowledgments This research has been supported by the National Natural Science Foundation of China (No. 51208206), Guangdong Provincial Department of Science (No. 2012A032300015), Guangdong Natural Science Foundation (No. S2011040000389), and the Fundamental Research Funds for the Central Universities (2013ZZ0031).

References

1. Y. Dong, J. Chen, C. Li, H. Zhu, *Dyes Pigm.* **73**(2), 261–268 (2007)
2. Y. Peng, D. Fu, R. Liu, F. Zhang, X. Liang, *Chemosphere* **71**(5), 990–997 (2008)
3. A. Azam, A. Hamid, *J. Hazard. Mater.* **133**(1–3), 167–171 (2006)
4. K.C. Chen, J.Y. Wu, C.C. Huang, Y.M. Liang, S.C.J. Hwang, *J. Biotechnol.* **101**(3), 241–252 (2003)
5. L. Abramian, H. El-Rassy, *Chem. Eng. J.* **150**(2–3), 403–410 (2009)
6. X.R. Xu, X.Z. Li, *Sep. Purif. Technol.* **72**(1), 105–111 (2010)
7. C.I. Pearee, J.R. Lloyd, J.T. Guthrie, *Dyes Pigm.* **58**(3), 179–196 (2003)
8. A.L. Teel, C.R. Warberg, D.A. Atkinson, R.J. Watts, *Water Res.* **35**(4), 977–984 (2001)
9. M.M. Huber, S. Canonica, G.Y. Park, U.V. Gunten, *Environ. Sci. Technol.* **37**(5), 1016–1024 (2003)

10. S.K. Ling, S.B. Wang, Y.L. Peng, J. Hazard. Mater. **178**(1–3), 385–389 (2010)
11. P. Neta, R.E. Huie, A.B. Ross, J. Phys. Chem. **17**, 1027–1082 (1998)
12. G.V. Buxton, C.L. Greenstock, W.P. Helman, A.B. Ross, J. Phys. Chem. Ref. Data **17**(2), 513–886 (1988)
13. M.G. Antoniou, A.A. de la Cruz, D.D. Dionysiou, Appl. Catal. B Env. **96**(3–4), 290–298 (2010)
14. D. Salari, A. Niaei, S. Aber, M.H. Rasoulifard, J. Hazard. Mater. **166**(1), 61–66 (2009)
15. K.C. Huang, R.A. Couttenye, G.E. Hoag, Chemosphere **49**(4), 413–420 (2002)
16. C.J. Liang, Y.Y. Guo, Water Air Soil Pollut. **223**(7), 4605–4614 (2012)
17. S.Y. Yang, X. Yang, X.T. Shao, R. Niu, L.L. Wang, J. Hazard. Mater. **186**(1), 659–666 (2011)
18. M. Ahmad, A.L. Teel, R.J. Watts, Environ. Sci. Technol. **47**(11), 5864–5871 (2013)
19. V.N. Kislenco, A.A. Berlin, N.V. Litovehenko, Russ. J. Gen. Chem. **65**(2), 1092–1096 (1995)
20. S. Rodriguez, L. Vasquez, D. Costa, A. Romero, A. Santos, Chemosphere **101**, 86–92 (2014)
21. R. Ahmadi, M.H. Rasoulifard, M. Vahedpour, Fresenius Environ. Bull. **22**(11), 3140–3145 (2013)
22. A. Ghauch, A.M. Tuqan, N. Kibbi, S. Geryes, Chem. Eng. J. **213**, 259–271 (2012)
23. G.G. Anipsitakis, D.D. Dionysiou, Environ. Sci. Technol. **38**(13), 3705–3712 (2004)
24. S.Y. Oh, H.W. Kim, J.M. Park, C. Yoon, J. Hazard. Mater. **168**(1), 346–351 (2009)
25. H.Y. Liang, Y.Q. Zhang, S.B. Huang, I. Hussain, Chem. Eng. J. **218**, 384–391 (2013)
26. C.S. Liu, K. Shih, C.X. Sun, F. Wang, Sci. Total Environ. **416**, 507–512 (2012)
27. C.L. Hsueh, Y.H. Huang, C.C. Wang, C.Y. Chen, Chemosphere **58**(10), 1409–1414 (2005)
28. J.H. Sun, X.L. Wang, J.Y. Sun, R.X. Sun, S.P. Sun, L.P. Qiao, J. Mol. Catal. A Chem. **260**(1–2), 241–246 (2006)
29. S.P. Sun, C.J. Li, J.H. Sun, S.H. Shi, M.H. Fan, Q. Zhou, J. Hazard. Mater. **161**(2–3), 1052–1057 (2009)
30. C. Liang, C.F. Huang, N. Mohanty, R.M. Kurakalva, Chemosphere **73**(9), 1540–1543 (2008)
31. APHA, AWWA, WEF, APHA, Washington, DC, (1998)
32. X.R. Xu, Z.Y. Zhao, X.Y. Li, J.D. Gu, Chemosphere **55**(1), 73–79 (2004)
33. A. Stefansson, Environ. Sci. Technol. **41**(17), 6117–6123 (2007)
34. O.S. Furman, A.L. Teel, R.J. Watts, Environ. Sci. Technol. **44**(16), 6423–6428 (2010)
35. C. Cai, H. Zhang, X. Zhong, L.W. Hou, Water Res. **66**, 473–485 (2014)
36. H. Hori, A. Yamamoto, E. Hayakawa, S. Taniyasu, N. Yamashita, S. Kutsuna, Environ. Sci. Technol. **39**(7), 2383–2388 (2005)
37. W. Chu, T.K. Lau, S.C. Fung, J. Agric. Food Chem. **54**(26), 10047–10052 (2006)
38. X.Y. Yu, Z.C. Bao, J.R. Barker, J. Phys. Chem. A **108**(2), 295–308 (2004)
39. C.J. Liang, C.F. Huang, Y.J. Chen, Water Res. **42**(15), 4091–4100 (2008)
40. R.V. Eldik, G.M. Harris, Inorg. Chem. **19**(4), 880–886 (1980)
41. K.F. Chen, C.M. Kao, L.C. Wu, R.Y. Surampalli, S.H. Liang, Water Environ. Res. **81**(7), 687–694 (2009)
42. S.H. Liang, C.M. Kao, Y.C. Kuo, K.F. Chen, J. Hazard. Mater. **185**(2–3), 1162–1168 (2011)
43. C.J. Liang, H.W. Su, Ind. Eng. Chem. Res. **48**(11), 5558–5562 (2009)
44. C.J. Liang, Z.S. Wang, C.J. Bruell, Chemosphere **66**(1), 106–113 (2007)
45. M.E. Lindsey, M.A. Tarr, Environ. Sci. Technol. **34**(3), 444–449 (2000)
46. F. Ji, C. Li, L. Deng, Chem. Eng. J. **178**, 239–243 (2011)
47. Y.L. Nie, C. Hu, J.H. Qu, X. Zhao, Appl. Catal. B **87**(1–2), 30–36 (2009)
48. T. Aman, A.A. Kazi, M.U. Sabri, Q. Bano, Colloids Surf. B **63**(1), 116–121 (2008)